DOI: 10.61782/fa.2025.0120

AN ADVANCED BOUNDARY INTEGRAL FORMULATION FOR SOUND SCATTERED BY DEFORMING BODIES

Beatrice De Rubeis[1*] **Massimo Gennaretti**[1]
Giovanni Bernardini[1] **Caterina Poggi**[1]
[1] Roma Tre University, Rome, Italy, 00146

ABSTRACT

Sound scattering is a phenomenon that may deeply affect the acoustic environment generated by sound sources. Recent studies have shown that the predictions of the multi-harmonic signal scattered by a deforming body impinged by a monochromatic sound wave, determined by means of linear boundary integral formulations expressed in terms of acoustic pressure governed by the Ffowcs-Williams and Hawkings equation and velocity potential perturbations, give different results. This occurs because the nonlinear field terms neglected in these two formulations make significant but different contributions in the case of a moving boundary. This paper introduces a novel harmonic-balance, velocity-potential cascade solution approach for nonlinear sound scattering that takes into account the effects of the flow-field produced by the dynamic deformation of the scatterer. The numerical investigation considers a pulsating sphere as sound scatterer impinged by a plane wave. It examines the convergence rate of the proposed nonlinear solution algorithm and the effects of the contributions related to the fluid flow generated by the surface pulsations on the scattered signal. The influence of the amplitude of the incident signal on the directivity pattern of the scattered sound is also investigated.

Keywords: *sound scattering, deforming scatterer, deformable-boundary integral formulation, boundary element method.*

****Corresponding author***: *beatrice.derubeis@uniroma3.it.*

1. INTRODUCTION

In the last decades, the aviation industry has experienced an exponential growth of vehicle configurations that may potentially be of great interest for the new concepts of air mobility. These include Urban Air Mobility (UAM) applications that might represent a solution to city traffic and pollution. However, unresolved issues like environmental impact in terms of both chemical and acoustic pollution must be faced to make the UAM a viable scenario [1].

Regarding the acoustic issue, it is of crucial importance to include acoustics since the earliest vehicle's design phases, so as to minimize the acoustic nuisance. National and international committees have established quantitative goals [2] in line with the Flightpath 2050 vision [3]. To achieve these targets, advanced and reliable methods and efficient computational tools for acoustic prediction must be developed and made available to researchers and designers.

The aeroacoustics of innovative vehicle configurations may be affected by phenomena that might be negligible in conventional concepts. For instance, the significant aerodynamic interactions occurring in distributed-propulsion systems [4, 5], and the body deformation affecting aerodynamics and aeroacoustics of highly flexible innovative configurations [6, 7], are among them. At the same time, the presence of the vehicle's airframe can significantly modify the noise radiated by the propulsive system, making the investigation of the installation effects of primary importance. This effect may be efficiently investigated by using scattering formulations.

These are based on the assumption that the impinging pressure wave is independent of the presence of the scatterer surface. This assumption allows the decomposition of the total pressure field into an incident and a scattered component, which can be solved separately, avoiding demanding computations where both the source and the scatterer are solved jointly. Indeed, first, the incident field is evaluated assuming the source as it was isolated and "frozen", with the rest of the vehicle components contributing only as scatterers.

A wide range of literature on this topic is available which typically assumes the scatterer as a rigid fixed or moving body (see, for instance, Refs. [8,9]). Formulations based on the acoustic field described in terms of either the velocity potential or the acoustic pressure governed by the Lighthill equation or the Ffowcs Williams and Hawkings equation (FWHE) have been developed (see, for instance, Refs. [10–13]).

However, over the past decades also the problem of sound scattered by deforming surfaces has been investigated. Considering the deformation of bodies of simple shape (like cylinders and spheres), Censor proposed the analytical solution of the scattered sound through a methodology based on a perturbation scheme applied to the linear wave equation [14, 15]. He showed that the nonlinear boundary conditions produce a multi-harmonic spectrum depending on the motion of the scatterer and the perturbation order included [14, 15].

A second possible source of multiple tones resides in the fluid nonlinearities which are strongly related to the deformation of the scatterer. The effect of fluid nonlinearities on the scattered field was studied, for instance, in Ref. [16] for an infinitely long cylinder impinged by a plane wave. The relative importance of the two sources of multi-harmonic scattering was examined by Mujica et al. [17].

In this context, this paper introduces a novel harmonic-balance, velocity-potential solution approach for nonlinear sound scattering that takes into account the effects of the flow-field produced by the dynamic deformation of arbitrarily shaped scatterers (nonlinearities arising from both boundary conditions and fluid flow are included in the analysis).

Specifically, the scattered noise field is described as the superposition of incremental velocity potential corrections which include progressively decreasing nonlinear field effects given by the combination of incident and scattered signal with flow-field generated by the motion of the scatterer (here called velocity potential cascade solution). Each incremental velocity potential contribution is determined through the application of a deformable-boundary integral formulation for wave equation solution recently developed by the authors [18].

The velocity potential cascade solution procedure is described in Sect. 2, while the harmonic-balance, frequency-domain numerical solution algorithm based on a boundary element method for the spatial discretization is outlined in Sect. 3. The results of a numerical investigation are discussed in Sect. 4. They regard the sound scattered by a pulsating sphere impinged by a plane sound wave. The numerical investigation examines the convergence rate of the proposed nonlinear solution algorithm and the effects of the fluid flow generated by surface pulsations on the scattered signal. The influence of the amplitude of the incident signal on the directivity pattern of the scattered sound is also investigated.

2. NONLINEAR INTEGRAL FORMULATION FOR SOUND SCATTERED BY DEFORMING BODIES

Let us consider a body moving in a perfect, inviscid gas, initially at rest, and express the generated irrotational fluid velocity field, $\mathbf{u}$, through the velocity potential φ such that $\mathbf{u} = \nabla\varphi$. Combining the mass conservation equation with Bernoulli's theorem for isentropic flows, the following inhomogeneous wave equation governing the velocity potential is obtained

$$\nabla^2\varphi - \frac{1}{c_0^2}\frac{\partial^2\varphi}{\partial t^2} = \sigma \tag{1}$$

where c_0 is the speed of sound of the undisturbed fluid and σ is the non-linear forcing term that is given by

$$\begin{aligned}\sigma = &\left[(c_0^2 - c^2)\nabla^2\varphi + 2\nabla\varphi\cdot\nabla\dot{\varphi}\right]/c_0^2 \\ &+ \left[\nabla\varphi\cdot\nabla(u^2)/2\right]/c_0^2\end{aligned} \tag{2}$$

where c is the local speed of sound and $\dot{(\,)} = \partial/\partial t$.

The differential problem is completed by the boundary condition of perturbation potential vanishing infinitely far from the moving body ($\varphi \to 0$ as $\mathbf{x} \to \infty$) and the imposition of impermeability of the body surface

$$\nabla\varphi\cdot\mathbf{n} = \mathbf{v}\cdot\mathbf{n} = \chi, \qquad \mathbf{x} \in \mathcal{S} \tag{3}$$

where $\mathbf{n}$ is the unit vector normal to the surface $\mathcal{S}$ of the scattering body, and $\mathbf{v}$ represents its velocity.

As demonstrated by the methodology presented in Ref. [18], the solution of Eqn. (1) for the velocity potential around moving and deforming bodies can be expressed through the following boundary integral formulation

$$\frac{1}{2}\varphi(\mathbf{x}_*,t_*) = \iint_\Omega \left[(1-M_n^2)\,\chi\,G_0\right] J\Big|_\theta \mathrm{d}\xi^1\mathrm{d}\xi^2$$
$$+\iint_\Omega \left[-M_n\mathbf{M}\cdot\nabla_t\varphi\,G_0\right] J\Big|_\theta \mathrm{d}\xi^1\mathrm{d}\xi^2$$
$$-\iint_\Omega \left[\varphi\frac{\partial G_0}{\partial n} - \frac{\partial\varphi}{\partial t}\Big|_\xi \frac{M_n}{c_0}G_0\right] J\Big|_\theta \mathrm{d}\xi^1\mathrm{d}\xi^2$$
$$-\iint_\Omega \frac{1}{\Theta}\frac{\partial}{\partial t}\Big|_\xi \left[\varphi\,G_0\,J\left(\frac{\mathbf{e}_r\cdot\mathbf{n}}{c_0} - \frac{M_n}{c_0}\right)\right]\Big|_\theta \mathrm{d}\xi^1\mathrm{d}\xi^2$$
$$+\iiint_{\mathcal{V}_\Omega} \sigma\,G_0\,J\Big|_\theta \mathrm{d}\xi^1\mathrm{d}\xi^2\mathrm{d}\xi^3 \qquad (4)$$

where (ξ^1,ξ^2,ξ^3) is a system of curvilinear coordinates defined over the body surface and the region around it. Ω and $\mathcal{V}_\Omega$ denote, respectively, the domains in the (ξ^1,ξ^2)-space and the (ξ^1,ξ^2,ξ^3)-space where the body surface and the neighbouring fluid region are mapped. In addition, $G_0 = -1/(4\pi r)$ with $r = |\mathbf{x}_* - \mathbf{x}|$ denoting the distance between the emitting point $\mathbf{x}$ and the receiving point $\mathbf{x}_*$, $\mathbf{M} = \mathbf{v}/c_0$, $M_n = \mathbf{M}\cdot\mathbf{n}$, $\mathbf{e}_r = \mathbf{r}/r$, while $J = |\mathbf{a}_1\times\mathbf{a}_2\cdot\mathbf{a}_3|/(1-\mathbf{M}\cdot\mathbf{e}_r)$ is the Jacobian of the curvilinear coordinate transformation ($\mathbf{a}_k$ are the covariant base vectors related to (ξ^1,ξ^2,ξ^3)). The symbol $(...)|_\theta$ indicates that the integrands must be evaluated at time $t = t_* - \theta$, which is the instant at which the surface of the body emitted the signal that at time t_* reaches the observer.

2.1 Cascade solution approach of nonlinear velocity potential scattering

The solution of the complete nonlinear boundary integral formulation expressed in Eqn. (4) requires the evaluation of a field term. This is a critical problem in terms of computational cost of the numerical solution algorithm. If an iterative approach is applied, the contributions from the usually numerous volume elements must be computed at each iteration, until convergence. Instead, if a linearized formulation is introduced and a boundary-field integral equation is solved, the values of the unknown function over surface panels and volume elements is determined directly through inversion of a matrix which, however, is typically very large (see, for instance, Ref. [10]).

For acoustic problems characterized by the interaction between a travelling sound wave and a moving body, it is convenient to divide the potential field into an incident field, φ^I, related to the travelling wave (independent of the body), and a component due to the presence of the body, φ^B. The latter can be further considered as the superposition of the velocity potential perturbation generated by the motion of the body, φ_0, and the scattered potential, φ^S.

Previous research has demonstrated that the flow-field generated by the body motion may significantly affect the scattered field, and that its effects are taken into account by including the nonlinear field term in Eqn. (4) [10, 13].

The nonlinear problem is solved through the following approach consisting of an incremental convergence of the scattered potential field. First, the velocity potential perturbation due to the motion of the scatterer (reference potential), φ_0, is solved through the boundary integral formulation in Eqn. (4) with

$$\chi = \chi_0 = \frac{\partial\varphi_0}{\partial n} = \mathbf{v}\cdot\mathbf{n}$$

and the corresponding field term

$$\sigma = \sigma_0(\varphi_0)$$

Next the scattered velocity potential field induced by the incident field is decomposed into several subcomponents, namely

$$\varphi^S = \varphi_1^S + \varphi_2^S + \varphi_3^S + ...$$

such that

$$\varphi_1^S > \varphi_2^S > \varphi_3^S > ...$$

In particular, φ_1^S is obtained as solution of Eqn. (4) with

$$\chi = \chi_1 = \frac{\partial\varphi_1^S}{\partial n} = -\frac{\partial\varphi^I}{\partial n}$$

and the nonlinear term given by the incremental contribution due to φ^I as

$$\sigma = \sigma_1(\varphi_0,\varphi^I) - \sigma_0(\varphi_0)$$

Therefore φ_1^S represents the component of the scattered field forced by the incident wave both through the impermeability boundary conditions (the dominating term) and the nonlinear field terms. The contribution of φ_1^S to σ_1 is omitted so as to have known field terms. However, once φ_1^S is evaluated, its incremental contribution to σ is used as a known term which produces the second element of the scattered potential series, φ_2^S. Specifically, φ_2^S is obtained as solution of Eqn. (4) with

$$\chi = \chi_2 = \frac{\partial\varphi_2^S}{\partial n} = 0$$

(note that the impermeability condition is satisfied by the combination of φ_0 and φ_1^S) and the nonlinear term as given by the following incremental contribution

$$\sigma = \sigma_2(\varphi_0, \varphi^I, \varphi_1^S) - \sigma_1(\varphi_0, \varphi^I)$$

Therefore φ_2^S represents the first correction to the scattered potential due to the nonlinear contributions of the scattered potential.

This procedure is repeated until the $j-$th incremental correction of the scattered velocity potential, φ_j^S, obtained as solution of Eqn. (4) with

$$\chi = \chi_j = \frac{\partial \varphi_j^S}{\partial n} = 0$$

and

$$\begin{aligned} \sigma \;&=\; \sigma_j(\varphi_0, \varphi^I, \varphi_1^S, ..., \varphi_{j-1}^S) \\ &-\; \sigma_{j-1}(\varphi_0, \varphi^I, \varphi_1^S, ..., \varphi_{j-2}^S) \end{aligned}$$

becomes negligible. It produces a cascade of incremental scattered potential fields whose superposition yields the total scattered field, φ^S.

3. VELOCITY POTENTIAL CASCADE BEM SOLUTION THROUGH HARMONIC BALANCE

For the purpose of the numerical application of the above boundary integral formulation, the surface of the body is discretized into N_p quadrilateral panels, while M_v volume elements are used to discretize the fluid domain where the field integral is evaluated. In these surface panels and volume elements the velocity potential and its space and time derivatives are assumed to be uniformly distributed, equal to those evaluated at their centroids (zeroth-order Boundary Element Method, BEM).

When the formulation in Eqn. (4) is applied as a boundary integral equation with known field contributions (as for the solutions of the scattered potential cascade), the satisfaction of the equation is imposed at the center of each surface discretization panel (collocation method). This yields the following set of algebraic equations whose solution provides the piecewise constant values of the velocity potential over the surfaces of the panels

$$\begin{aligned} &\frac{1}{2}\varphi_k(t_*) = \sum_{i=1}^{N_p} A_{ki}\chi_i(t_* - \theta_{ki}) \\ &+ \sum_{i=1}^{N_p} B_{ki}\varphi_i(t_* - \theta_{ki}) + \sum_{i=1}^{N_p} C_{ki}\dot{\varphi}_i(t_* - \theta_{ki}) \\ &+ \sum_{i=1}^{N_p} F_{ki}\varphi_i^t(t_* - \theta_{ki}) + \sum_{m=1}^{M_v} H_{km}\sigma_m(t_* - \theta_{km}) \end{aligned} \tag{5}$$

where φ_i and χ_i denote, respectively, the velocity potential and the function χ evaluated at the center of the i-th panel, φ^t is the derivative of the velocity potential along the direction of the local body Mach number component tangent to the surface, $\mathbf{M}_t$, θ_{ki} represents the signal transmission delay θ related to the observer at the center of the k-th panel and the emitting source at the center of the i-th panel, while σ_m is the nonlinear forcing therm evaluated at the center of the m-th volume. The influence coefficients are defined as

$$A_{ki} = \iint_{\Omega_i} (1 - M_n^2)\, G_0\, \hat{J}\,\Big|_{\theta_{ki}} \mathrm{d}\xi^1 \mathrm{d}\xi^2$$

$$B_{ki} = \iint_{\Omega_i} \left[-\frac{\partial G_0}{\partial n}\,\hat{J} + \frac{1}{\Theta}\frac{\partial}{\partial \tau}\Big|_{\xi} (G_0\,\Lambda) \right]\Big|_{\theta_{ki}} \mathrm{d}\xi^1 \mathrm{d}\xi^2$$

$$C_{ki} = \iint_{\Omega_i} \left[\frac{M_n}{c_0} G_0\,\hat{J} + G_0 \frac{\Lambda}{\Theta} \right]\Big|_{\theta_{ki}} \mathrm{d}\xi^1 \mathrm{d}\xi^2$$

$$F_{ki} = -\iint_{\Omega_i} M_n\, M_t\, G_0\,\hat{J}\,\Big|_{\theta_{ki}} \mathrm{d}\xi^1 \mathrm{d}\xi^2$$

$$H_{km} = \iiint_{\mathcal{V}_{\Omega_m}} G_0\,\hat{J}\,\Big|_{\theta_{km}} \mathrm{d}\xi^1 \mathrm{d}\xi^2 \mathrm{d}\xi^3$$

where $\Lambda = \hat{J}\,(-\mathbf{e}_r \cdot \mathbf{n} + M_n)/c_0$, with $\hat{J} = J/|\Theta|$, and $\Omega_i, \mathcal{V}_{\Omega_m}$ denoting, respectively, the (ξ^1, ξ^2)-domain and the (ξ^1, ξ^2, ξ^3)-domain where the surface of the i-th panel and the volume of the m-th field element are mapped. The factor $1/2$ which appears at the left-hand side of Eqn. (4) and Eqn. (5) accounts for the contribution of the free terms deriving from the singularity of the kernel function $\partial G_0/\partial n$ arising when the position of the observer tends to the limit on the emitting surface. Thus, when $k = i$ the coefficients B_{ki} are intended as Cauchy principal values of the surface integral [19, 20].

Once the velocity potential over the sphere is known, it may be readily used to determine the velocity potential field radiated at external points, through application of the discretized boundary integral representation formally identical to Eqn. (5), with the factor $1/2$ at the left-hand side removed [19, 20]. This is necessary, for instance, for the evaluation of the potential field at the centroids of the discretization volumes for the definition of the field forcing terms in the cascade solution process).

3.1 Multi-harmonic scattering solution algorithm

The integral formulation in Eqn. (4) is expressed in the time domain. However, acoustic problems are typically represented in the frequency domain because acoustic phenomena typically deal with high-frequency signals, for which time-domain solution algorithms are subject to the occurrence of numerical instabilities that prevent the evaluation of accurate and reliable solutions (see, for instance, Ref. [21]).

Considering an arbitrarily deforming scatterer in arbitrary motion, the above coefficients of the BEM formulation are time-varying. To determine a frequency-domain expression of the scattered field, let us assume that the incident velocity potential is harmonic and that the influence coefficients are periodic, with their fundamental harmonic being a multiple or a sub-multiple of the harmonic of the incident signal. Note that this assumption is not too limiting or unrealistic. It is applicable, for example, in all those cases where the deformation of the scatterer is the result of the response of an elastic structure to incident velocity potential.

Thus, following the approach introduced in Ref. [21], it is convenient to express the velocity potential at each centroid of the discretized BEM domain in terms of its Fourier series as

$$\begin{aligned}\varphi(t_* - \theta) = \varphi_0 \quad &+ \quad \sum_{n=1}^{N_a} \varphi_{nc} \cos\left[n\omega(t_* - \theta)\right] \\ &+ \quad \sum_{n=1}^{N_a} \varphi_{ns} \sin\left[n\omega(t_* - \theta)\right]\end{aligned}$$

where ω represents the fundamental harmonic, N_a is the number of harmonics included in the analysis, φ_{nc} and φ_{ns} are the cosine and sine components of the n-th harmonic of the velocity potential, while φ_0 denotes its average value.

The combination of this expression of the velocity potential at the centroids of the discretization elements with Eqn. (5), followed by the determination of the Fourier series expansion of the coefficients of the resulting set of algebraic equations, and by the balancing of the left-hand-side and right-hand-side harmonics yields the solution (see Ref. [21] for details)

$$\boldsymbol{\varphi} = (\mathbf{I} - \mathbf{D})^{-1}\mathbf{f} \tag{6}$$

where

$$\boldsymbol{\varphi} = \begin{bmatrix} \boldsymbol{\varphi}_0 \\ \boldsymbol{\varphi}_{1c} \\ \boldsymbol{\varphi}_{1s} \\ \vdots \\ \boldsymbol{\varphi}_{N_a c} \\ \boldsymbol{\varphi}_{N_a s} \end{bmatrix}, \quad \mathbf{f} = \begin{bmatrix} \mathbf{f}_0^\chi + \mathbf{f}_0^\sigma \\ \mathbf{f}_{1c}^\chi + \mathbf{f}_{1c}^\sigma \\ \mathbf{f}_{1s}^\chi + \mathbf{f}_{1s}^\sigma \\ \vdots \\ \mathbf{f}_{N_a c}^\chi + \mathbf{f}_{N_a c}^\sigma \\ \mathbf{f}_{N_a s}^\chi + \mathbf{f}_{N_a s}^\sigma \end{bmatrix}$$

with $\boldsymbol{\varphi}_{nc}$ denoting, for instance, the vector collecting the n-th cosine components of the velocity potentials at the N_p centroids, while $\mathbf{f}_{nc}^\chi$ and $\mathbf{f}_{nc}^\sigma$ are vectors collecting the n-th cosine components of the forcing terms deriving, respectively, from the Neumann boundary condition, *i.e.,* given by

$$f_k^\chi(t_*) = \sum_{i=1}^{N_p} A_{ki}\chi_i(t_* - \theta_{ki})$$

and from the nonlinear field contributions, *i.e.,* given by

$$f_k^\sigma(t_*) = \sum_{m=1}^{M_v} H_{km}\sigma_m(t_* - \theta_{km})$$

The matrix $\mathbf{D}$ is a square matrix of dimensions $N_p(2N_a + 1) \times N_p(2N_a + 1)$, whose entries are the Fourier components of the time-varying coefficients of the set of algebraic equations obtained by combining the Fourier series expansion of the velocity potential with Eqn. (5) (see Ref. [21] for details).

In the present problem of sound scattered by deforming bodies, this solution procedure is used to determine φ_0 and the incremental scattering components $\varphi_1^S, \varphi_2^S, \ldots$ (it is worth underlying that the results presented in Ref. [21] correspond to the first scattering component, φ_1^S, under the assumption of neglecting the effects of the reference potential, φ_0).

Finally, note that it can be applied to an arbitrarily deforming body by representing impinging wave and body motion through suitable discrete Fourier transforms and determining the solution by combining the corresponding harmonic components.

4. NUMERICAL RESULTS

All numerical results presented in the following regard applications to a pulsating spherical scatterer. They are obtained through a discretization of the surface that ensures converged solutions. Specifically, as a result of a preliminary investigation of numerical convergence, the discretization panels used are $N_p = 600$, generated by dividing the sphere surface through 30 meridians and 20 parallels. The number of harmonics, N_a, considered in the solution algorithm depends on the problem examined. Converged results are obtained by increasing N_a until the significant harmonics of the output remain unchanged.

We consider a sphere of radius $r_0 = 1$ m subject to pulsations of amplitude $a_d = 0.2r_0$ and frequency, ω_d, such that $k_d r_0 = 0.3$ (with $k_d = \omega_d/c_0$ denoting the deformation wave number), impinged by a plane wave, φ^I, of amplitude A_I and wave number $k_I = k_d$. It is possible to show that in this case $\sigma_0(\varphi_0) \approx 0$.

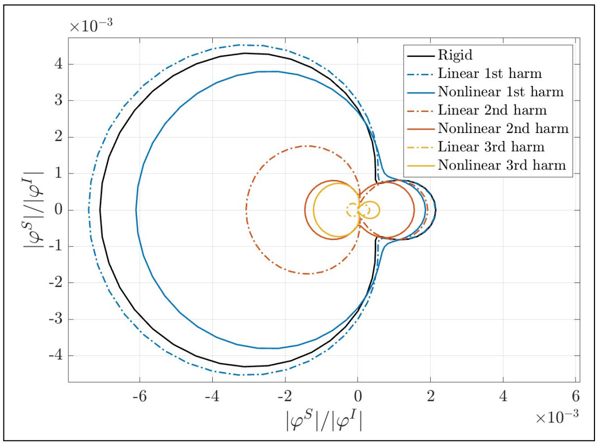

Figure 1. Multi-harmonic directivity patterns of the scattered signal provided by linear and nonlinear solutions. $A_I = 1$ m^2/s, $d/r_0 = 10$.

Figure 1 presents the directivity patterns of the first three harmonics of the scattered signal evaluated on a set of microphones located on a circle at a distance $d = 10r_0$ from the sphere centre, and lying on a plane perpendicular to the plane of the impinging wave. In particular, it compares the results obtained by the linear formulation introduced in Ref. [21] (equivalent to the first contribution to the present cascade solution, φ_1^S, when the effects of φ_0 are neglected), with the proposed nonlinear solution which includes the distortion effects due to the flow generated by pulsations. In addition, the mono-harmonic solution for the rigid sphere is depicted. This figure proves that the fluid flow generated by sphere pulsations may produce significant distortion to the scattered signal which cannot be neglected.

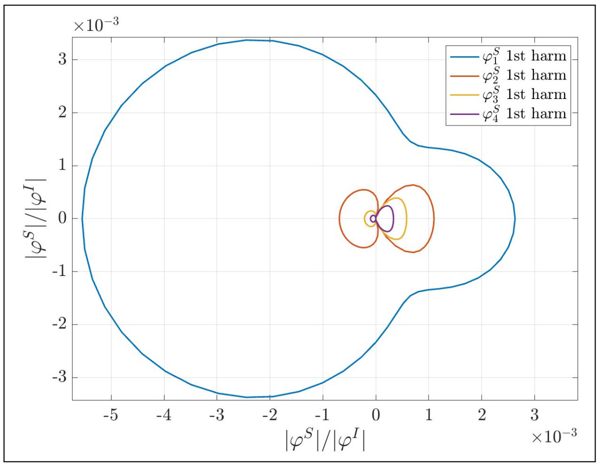

Figure 2. Directivity patterns of the first harmonic of the scattered signal cascade components. $A_I = 1$ m^2/s, $d/r_0 = 10$.

Next, Figs. 2-4 show the contributions of the different cascade components to the directivity patterns of the first three harmonics of the scattered signal. They demonstrate the rapid decrease of the contributions from the cascade components with the increase of iterations, and hence the fast convergence rate of the applied algorithm for the nonlinear solution.

Finally, the role played by the amplitude of the incident sound wave in nonlinear scattering is examined. In particular, Figs. 5 and 6 present the comparison between the multi-harmonic directivity patterns provided by the present nonlinear solution and the linearized one introduced in Ref. [10], respectively for $A_I = 1$ m^2/s and $A_I = 10$ m^2/s (note that the linearized solution given by the boundary-field formulation of Ref. [10] can be equivalently obtained by the present approach by including only linear contributions of φ^I and φ^S in σ). These figures prove that, for the ratio between the scattered field and the incident sound wave: (i) for low-amplitude incident sound waves, linearized and nonlinear solutions are fully equivalent; (ii) the linearized solution is (as expected) independent of the amplitude of the incident wave; (iii) the nonlinear solution differs from the linearized one as the amplitude of the incident wave increases.

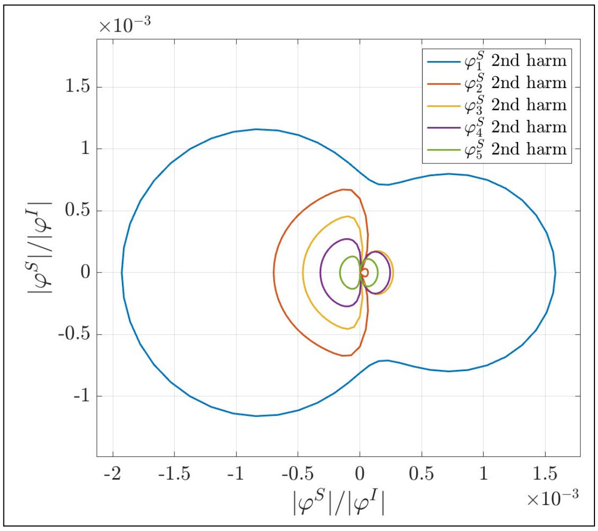

Figure 3. Directivity patterns of the second harmonic of the scattered signal cascade components. $A_I = 1$ m^2/s, $d/r_0 = 10$.

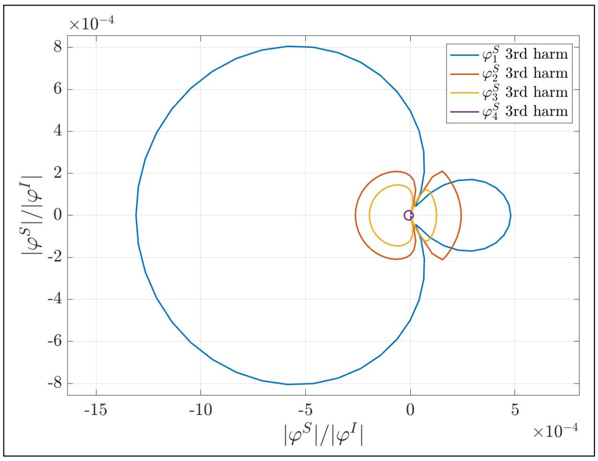

Figure 4. Directivity patterns of the third harmonic of the scattered signal cascade components. $A_I = 1$ m^2/s, $d/r_0 = 10$.

5. CONCLUDING REMARKS

A novel harmonic-balance, velocity-potential cascade solution approach for nonlinear sound scattering has been introduced. It takes into account the effects of the flow-field produced by the dynamic deformation of the scatterer. For a pulsating sphere impinged by a plane sound wave, the numerical investigation has proven that: (i) the

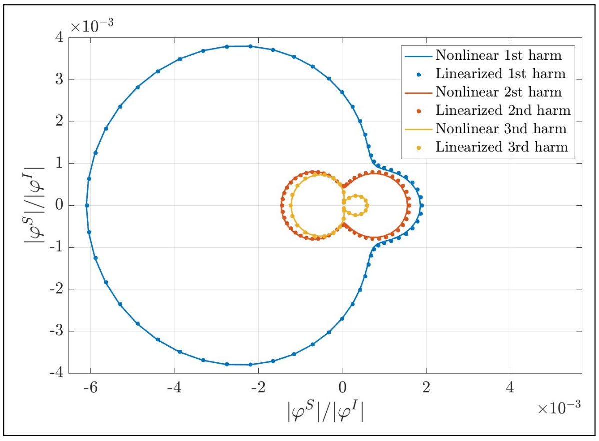

Figure 5. Multi-harmonic directivity patterns of the scattered signal provided by linearized and nonlinear solutions. $A_I = 1$ m^2/s, $d/r_0 = 10$.

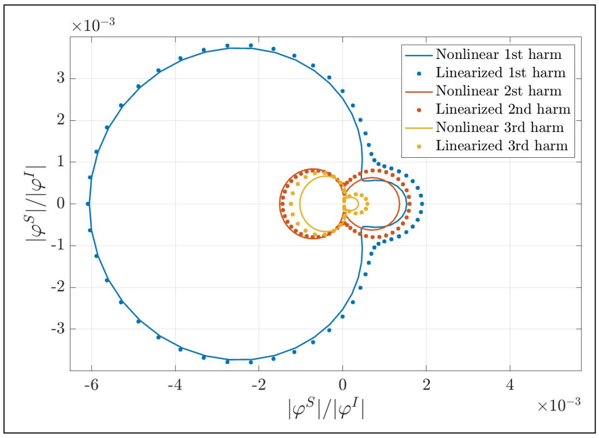

Figure 6. Multi-harmonic directivity patterns of the scattered signal provided by linearized and nonlinear solutions. $A_I = 10$ m^2/s, $d/r_0 = 10$.

proposed harmonic-balance cascade prediction algorithm is able to provide a rapidly-converged nonlinear scattered solution; (ii) for large-amplitude, non-small frequency pulsations of the sphere the nonlinear solution significantly differ from the linear one; (iii) for small-amplitude incident sound waves, linearized and nonlinear solutions are fully equivalent; (iv) as the amplitude of the incident wave increases linearized and nonlinear solutions differ, thus showing that accurate analyses of sound scattered by deforming bodies require the application of a nonlinear solution approach like that proposed in the present work.

6. REFERENCES

[1] S. A. Rizzi, D. L. Huff, D. D. Boyd, P. Bent, B. S. Henderson, K. A. Pascioni, D. C. Sargent, D. L. Josephson, M. Marsan, H. B. He, *et al.*, "Urban air mobility noise: Current practice, gaps, and recommendations," tech. rep., 2020.

[2] ICAO, "Environmental report 2016," tech. rep., International Civil Aviation Organization, 2016.

[3] EC, "Flightpath 2050, europe's vision for aviation," tech. rep., European Commission, 2011.

[4] C. Poggi, G. Bernardini, M. Gennaretti, and R. Camussi, "Scalability of mach number effects on noise emitted by side-by-side propellers," *Applied Sciences*, vol. 12, no. 19, p. 9507, 2022.

[5] C. Poggi, M. Rossetti, J. Serafini, G. Bernardini, M. Gennaretti, and U. Iemma, "Neural network meta–modelling for an efficient prediction of propeller array acoustic signature," *Aerospace Science and Technology*, vol. 130, p. 107910, 2022.

[6] Q. Ai, M. Azarpeyvand, X. Lachenal, and P. M. Weaver, "Aerodynamic and aeroacoustic performance of airfoils with morphing structures," *Wind Energy*, vol. 19, no. 7, pp. 1325–1339, 2016.

[7] Z. Kan, D. Li, S. Zhao, J. Xiang, and E. Sha, "Aeroacoustic and aerodynamic characteristics of a morphing airfoil," *Aircraft Engineering and Aerospace Technology*, vol. 93, no. 5, pp. 888–899, 2021.

[8] H. A. Schenck, "Improved integral formulation for acoustic radiation problems," *The Journal of the Acoustical Society of America*, vol. 44, no. 1, pp. 41–58, 1968.

[9] D. Colton and R. Kress, *Integral equation methods in scattering theory*. SIAM, 2013.

[10] M. Gennaretti, G. Bernardini, C. Poggi, and C. Testa, "Velocity-potential boundary-field integral formulation for sound scattered by moving bodies," *AIAA Journal*, vol. 56, no. 9, pp. 3547–3557, 2018.

[11] G. Bernardini, C. Poggi, M. Gennaretti, and C. Testa, "Study of velocity-potential integral formulations for sound scattered by moving bodies," *AIAA Journal*, vol. 59, no. 3, pp. 1008–1019, 2021.

[12] M. Gennaretti and C. Testa, "A boundary integral formulation for sound scattered by elastic moving bodies," *Journal of Sound and Vibration*, vol. 314, no. 3-5, pp. 712–737, 2008.

[13] C. Testa, C. Poggi, G. Bernardini, and M. Gennaretti, "Pressure-field permeable-surface integral formulations for sound scattered by moving bodies," *Journal of Sound and Vibration*, vol. 459, p. 114860, 2019.

[14] D. Censor, "Scattering of a sound wave by a vibrating surface," *Journal of Sound and Vibration*, vol. 25, no. 1, pp. 101–110, 1972.

[15] D. Censor, "Harmonic and transient scattering from time varying obstacles," *The Journal of the Acoustical Society of America*, vol. 76, no. 5, pp. 1527–1534, 1984.

[16] J. C. Piquette and A. L. Van Buren, "Nonlinear scattering of acoustic waves by vibrating surfaces," *The Journal of the Acoustical Society of America*, vol. 76, no. 3, pp. 880–889, 1984.

[17] N. Mujica, R. Wunenburger, and S. Fauve, "Scattering by time varying obstacles," *The European Physical Journal B-Condensed Matter and Complex Systems*, vol. 33, pp. 209–213, 2003.

[18] M. Gennaretti, B. De Rubeis, C. Poggi, and G. Bernardini, "Deformable-boundary integral formulation for the solution of arbitrarily-forced acoustic wave equation," *Journal of Sound and Vibration*, vol. 591, p. 118618, 2024.

[19] L. Morino and M. Gennaretti, "Boundary integral equation methods for aerodynamics," *in: Computational nonlinear mechanics in aerospace engineering (editor S. N. Atluri), Progress in Aeronautics and Astronautics, Washington, AIAA, Inc.*, pp. 279–320, 1992.

[20] M. Gennaretti, *Fundamentals of Aeroelasticity*. Springer Nature, Switzerland AG, 2024.

[21] B. De Rubeis, M. Gennaretti, C. Poggi, and G. Bernardini, "Sound scattered by deforming bodies through boundary integral formulations," *AIAA Journal*, 2025.